

Composite Control and Co-Simulation in In-Wheel Motor Electric Vehicle Suspension

Jialing Yao^{*,1,2}, Shuhui Ding¹, Zhaochun Li³, Shan Ren¹, Saied Taheri², Zhongnan Zhang¹

¹College of Automobile and Traffic Engineering, Nanjing Forestry University, Nanjing, 210037, China

²Center for Tire Research, Mechanical Engineering Department, Virginia Polytechnic Institute and State University, Blacksburg, VA 24060, USA

³College of Mechanical and Electronic Engineering, Nanjing Forestry University, Nanjing, 210037, China

Abstract: An in-wheel motor electric vehicle has high unsprung mass because of its in-wheel motor, which decreases vehicle ride comfort and vehicle safety. This paper presents a controllable suspension employing an optimal design hybrid damping control strategy based on ideal skyhook and groundhook as a reference. A sliding mode controller is designed to make the plant track the ideal reference model. The exponent reaching law based on fraction order calculus is used to improve the dynamic quality of the sliding mode motion. Moreover, a dynamics model of in-wheel motor electric vehicle suspension is established in Adams. The joint simulation of Adams and Matlab prove that the designed controller can reduce tire dynamic load effectively, maintain better ride comfort, and suppress vibration better than the integer order exponential reaching law. Furthermore, the proposed controller has better composite performance than the general hybrid damping control strategy.

Keywords: Fraction order sliding mode control, in-wheel motor, semi-active suspension, unsprung mass.

1. INTRODUCTION

An in-wheel motor electric vehicle can achieve four-wheel independent torque or speed control with good dynamics control and high utilization rate of space, effectively reducing the height of the center of the body to improve the security and stability of the vehicle. The in-wheel motor electric vehicle also has a flexible drive form, but it does not obtain market sales. An important constraint factor is its in-wheel motor, which brings with it an additional unsprung mass, aside from an immature motor and control technology. The in-wheel motor placed inside the wheel rim causes the unsprung mass to increase significantly, directly affecting the ground contact of the tire, road friendliness, and vehicle ride comfort [1-3].

Hredzak designed a disc-type motor [1] that transforms the stator into a sprung mass while the rotor drives the wheels through a long half-shaft. This motor has high power density, fast response, and small moment of inertia, and it has significant performance improvement in vehicle vertical vibration. However, the motor rotor and stator are easy to misplace, and this misplacement leads to magnetic field changes; therefore, it is difficult to design. Literature [4] transformed an unsprung mass into a sprung mass by using a special motor, thus reducing the negative influences caused by the unsprung mass. Bridgestone Corporation developed an in-wheel motor drive system with a dynamic vibration absorber outer rotor, which controls the negative influences

on the vertical vibration caused by the unsprung mass by building an absorber utilizing motor mass [5]. In [6], a similar method was adopted for further study. After the analysis of the dynamics for the suspension system, the motor was used as a mass-damper system to reduce the unsprung mass. Literature [7, 8] transformed the mass of the motor stator into a sprung mass by designing a special plane motor. In [9, 10], a direct drive system was designed and analyzed by using the advantages of the axial flux motor, such as high torque density, high power density, and no cogging effect. Mellor [11] sought ways to improve the vertical vehicle performance by integrating designs for the in-wheel motor, wheel rim, wheel hub, and other parts. Based on LQG optimal control theory and preview control methods between two axles, Ning [12] found ways to reduce the dynamic loads of the wheels for the non-steering-wheel double wishbone-torsion bar spring suspension system.

Reducing the vertical vibration negative influences induced by a high unsprung mass by improving the design of the in-wheel motors structure can be effective, but it has the disadvantages of having a too complex structure and a too large mass. An important research direction for developing a suspension system is to develop a suitable control strategy for a controllable suspension system for the in-wheel motor electric vehicle.

This paper presents a controllable suspension employing an optimally designed hybrid damping control strategy based on ideal skyhook and groundhook as a reference model to achieve a balance between comfort and safety. A sliding mode controller is designed to make the plant track the ideal reference model. The exponent reaching law based on fraction order calculus is used to improve the dynamic

quality of the sliding mode motion. The designed strategy uses magneto-rheological dampers as the actuator of a semi-active suspension system. The proposed control strategy aims to improve the ground contact of the tire and the comfort of an in-wheel motor electric vehicle.

2. MODELING OF A QUARTER-CAR WITH SEMI-ACTIVE SUSPENSIONS

2.1. Semi-Active Suspension Mathematical Model

This paper intends to reduce the tire dynamic load and maintain better ride comfort by designing a suitable control strategy for a controllable semi-active suspension system. Therefore, the internal structure of the in-wheel motor is not considered. The quarter-car two-degrees-of-freedom semi-active suspension model is shown in Fig. (1).

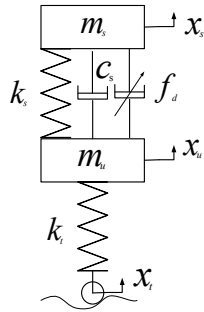


Fig. (1). Quarter-car semi-active suspension model.

According to Newton's second law, the semi-active suspension differential equation of motion can be written as:

$$\begin{cases} m_s \ddot{x}_s + k_s(x_s - x_u) + c_s(\dot{x}_s - \dot{x}_u) + f_d = 0 \\ m_u \ddot{x}_u - k_s(x_s - x_u) - c_s(\dot{x}_s - \dot{x}_u) + k_t(x_u - x_t) - f_d = 0 \end{cases} \quad (1)$$

where k_s is the suspension stiffness, k_t is the tire stiffness, c_s is the fixed damping, x_t is the vertical displacement of the ground (road input), x_s is the vertical displacement of the sprung mass, x_u is the vertical displacement of the unsprung mass, and f_d is the control force.

The state variables $x_{p1} = x_s - x_u$, $x_{p2} = \dot{x}_s$, $x_{p3} = x_u - x_t$, $x_{p4} = \dot{x}_u$ are selected. Equation (1) is rewritten as the following state equation:

$$\dot{X}_p = A_p X_p + B_{p1} f_d + B_{p2} \dot{x}_t = A_p X_p + B_p u_p \quad (2)$$

where,

$$A_p = \begin{bmatrix} 0 & 1 & 0 & -1 \\ -\frac{k_s}{m_s} & -\frac{c_s}{m_s} & 0 & \frac{c_s}{m_s} \\ 0 & 0 & 0 & 1 \\ \frac{k_s}{m_u} & \frac{c_s}{m_u} & -\frac{k_t}{m_u} & -\frac{c_s}{m_u} \end{bmatrix}, B_{p1} = \begin{bmatrix} 0 \\ -\frac{1}{m_s} \\ 0 \\ \frac{1}{m_u} \end{bmatrix}$$

$$B_{p2} = [0 \ 0 \ -1 \ 0]^T, B_p = \begin{bmatrix} B_{p1} & B_{p2} \end{bmatrix}, u_p = \begin{bmatrix} f_d \\ \dot{x}_t \end{bmatrix}$$

2.2. Semi-Active Suspension Multi-Body Model

The simplified model of the quarter-car in-wheel motor electric vehicle suspension is established in Adams/View. The following assumptions are made [13]:

- (1) All parts are considered to be rigid, the kinematic pair is a rigid connection, and the internal clearance is negligible.
- (2) A component that simulates the excitation caused by an uneven ground, which is directly in contact with the tire and connected with the ground *via* the prismatic pair. It can move up and down vertically.
- (3) The sprung mass and the unsprung mass can only move up and down vertically relative to the ground.

The simplified model of the suspension is shown in Fig. (2). The input and output variables are defined in Adams, which is the interface for data transferring with a control system designed in Matlab. The input variable in Adams is the control force applied to the body, and the output variables are body acceleration, wheel acceleration, suspension deflection, and wheel deflection. The required intermediate files are generated through the Adams/Control module.

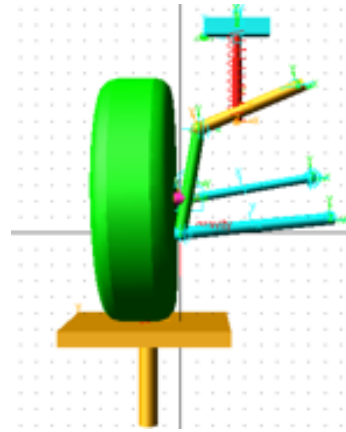


Fig. (2). Quarter-car multi-body model.

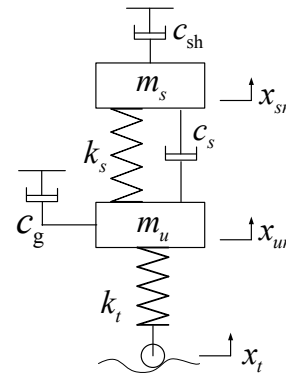


Fig. (3). Reference model with ideal hybrid control.

3. MODEL REFERENCE FRACTIONAL ORDER SLIDING MODE CONTROLLER (FOSMC) DESIGN

The model reference fractional order sliding mode controller is used to reduce the tire dynamic load of the in-wheel motor electric vehicle while maintaining vehicle ride comfort. An ideal skyhook and groundhook controllable suspension with optimal design damping for a quarter-car is used as the reference model. As shown in Fig. (3), the dynamic equations of the reference model can be obtained as

$$\begin{cases} m_s \ddot{x}_{sr} + k_s(x_{sr} - x_{ur}) + c_s(\dot{x}_{sr} - \dot{x}_{ur}) + c_{sh}\dot{x}_{sr} = 0 \\ m_u \ddot{x}_{ur} - k_s(x_{sr} - x_{ur}) - c_s(\dot{x}_{sr} - \dot{x}_{ur}) + k_t(x_{ur} - x_t) + c_g\dot{x}_{ur} = 0 \end{cases} \quad (3)$$

The state variables $x_{r1} = x_{sr} - x_{ur}$, $x_{r2} = \dot{x}_{sr}$, $x_{r3} = x_{ur} - x_t$, $x_{r4} = \dot{x}_{ur}$ are selected. Equation (3) is rewritten as the following state equation:

$$\dot{X}_r = A_r X_r + B_r u_r \quad (4)$$

where,

$$X_r = \begin{bmatrix} x_{r1} \\ x_{r2} \\ x_{r3} \\ x_{r4} \end{bmatrix}, A_r = \begin{bmatrix} 0 & 1 & 0 & -1 \\ -\frac{k_s}{m_s} & -\frac{c_{sh} + c_s}{m_s} & 0 & \frac{c_s}{m_s} \\ 0 & 0 & 0 & 1 \\ \frac{k_s}{m_u} & \frac{c_s}{m_u} & -\frac{k_t}{m_u} & -\frac{c_s + c_g}{m_u} \end{bmatrix}$$

$$B_r = [0 \ 0 \ -1 \ 0]', u_r = \dot{x}_t$$

Assume that the plant in Fig. (1) can track the reference model in Fig. (3), and design the control forces to make the tracking error $e = X_r - X_p$ meet

$$(1) \quad \lim_{t \rightarrow 0} e(t) = 0$$

$$(2) \quad e(t) \text{ has good dynamic quality}$$

If $rank\{B_p, (A_r - A_p)\} = rank(B_p, B_r) = rank(B_p)$, the tracking error meets the trace condition. The switching surface function can be set $s = Ce$.

$$\dot{s} = C\dot{e} = C[A_r e + (A_r - A_p)X_p + B_r u_r - B_p u_p] \quad (5)$$

The coefficient matrix C of the switching surface function can be obtained by using pole placement method. Therefore, we obtain the switching surface $s = Ce$. The equivalent control rate is

$$f_{deq} = (CB_{p1})^{-1} C[A_r e + (A_r - A_p)X_p] \quad (6)$$

To improve the dynamic quality of the sliding mode motion, the exponential reaching law with fraction order calculus was used in [14]. It is similar to the one proposed by Gao [15]:

$$D^\alpha s = -ks - \varepsilon \operatorname{sgn}(s), \quad 0 < \alpha < 1, \varepsilon > 0, k > 0 \quad (7)$$

The $1 - \alpha$ order derivative is

$$\dot{s} = D^{1-\alpha} D^\alpha s = D^{1-\alpha} (-ks - \varepsilon \operatorname{sgn}(s)) \quad (8)$$

then

$$f_d = (CB_{p1})^{-1} [C(A_r e + (A_r - A_p)X_p) + D^{1-\alpha}(ks + \dots \varepsilon \operatorname{sgn}(s))] = f_{deq} + (CB_{p1})^{-1} D^{1-\alpha}(ks + \varepsilon \operatorname{sgn}(s)) \quad (9)$$

In summary, the control force of the semi-active suspension is

$$f_d = \begin{cases} f_{deq} + (CB_{p1})^{-1} \\ D^{1-\alpha}(ks + \varepsilon \operatorname{sgn}(s)), \begin{bmatrix} f_{deq} + (CB_{p1})^{-1} \\ D^{1-\alpha}(ks + \varepsilon \operatorname{sgn}(s)) \end{bmatrix} (x_2 - x_{r2}) > 0 \\ 0 \quad \begin{bmatrix} f_{deq} + (CB_{p1})^{-1} \\ D^{1-\alpha}(ks + \varepsilon \operatorname{sgn}(s)) \end{bmatrix} (x_2 - x_{r2}) < 0 \end{cases} \quad (10)$$

When the fractional order exponent reaching law is calculated, the fractional order calculus proposed by Grünwald [16] is adopted:

$${}_c D_x^\alpha f(x) \stackrel{def}{=} \lim_{h \rightarrow 0} \frac{1}{h^\alpha} \sum_{j=0}^{[\frac{x-c}{h}] - 1} (-1)^j \binom{\alpha}{j} f(x - jh) \quad (11)$$

where $[\cdot]$ is the integer part of the value. The numerical calculation expression of the fractional derivative can be derived from the definition provided by Grünwald:

$${}_{[t-L]} D_t^\alpha f(t) \approx h^{-\alpha} \sum_{j=0}^N c_j f(t - jh) \quad (12)$$

where L is the memory length, h is the calculation steps, $N = \min\{\frac{t}{h}, \frac{L}{h}\}$, and c_j is the quadratic coefficient, which can be obtained by the following recursive formula:

$$c_0 = 0, \quad c_j = \left(1 - \frac{1 + \alpha}{j}\right) c_{j-1}$$

Therefore, the numerical solution of the fractional reaching law can be obtained as follows:

$$\begin{aligned} D^\alpha s(t_{n+1}) &\approx h^{-\alpha} \sum_{j=0}^N c_j f(t_{n+1} - jh) \\ &= h^{-\alpha} s(t_{n+1}) + h^{-\alpha} \sum_{j=1}^N c_j s(t_{n+1} - t_j) \end{aligned} \quad (13)$$

4. SIMULATION CALCULATION AND ANALYSIS

4.1. Optimal Matching of Suspension Parameters

The simulation is carried out with the B grade road model as the random input. The road roughness coefficient is $G_q(n_0) = 64 \times 10^{-6} \text{ m}^3$, the vehicle speed is $V = 20 \text{ m/s}$, the frequency of reference space is $n_0 = 0.1 \text{ m}^{-1}$, the sampling period is $t = 0.01 \text{ s}$, and the power spectral density (p.s.d.) of a band-limited white noise input is

$$G_q(f) = 4\pi^2 G_q(n_0) n_0^2 V$$

The magnetorheological damper is used as the actuator of the semi-active suspension. The mathematical model using the polynomial model [17, 18] is as follows:

$$f_d = \sum_{i=0}^n a_i v^i, \quad a_i = b_i + c_i I, \quad \text{then } f_d = \sum_{i=0}^n (b_i + c_i I) v^i \quad (14)$$

where f_d is the damping force, a_i is the coefficient of curve fitting, n is the polynomial number, and v is the speed of the damper piston.

The inverse model of the magneto-rheological damper is

$$I = \frac{f_d - \sum_{i=0}^n b_i v^i}{\sum_{i=0}^n c_i v^i} \quad (15)$$

The vehicle parameters are based on reference [19]: $m_s = 400\text{kg}$, $m_u = 48\text{kg}$ (Conventional suspension $m_u = 40\text{kg}$, increased by 20% here), $k_s = 15800\text{N/m}$, $k_t = 158000\text{N/m}$, and $c_s = 126\text{N}\cdot\text{s/m}$. To effectively reduce the tire dynamic load and maintain better ride comfort, selecting the parameters of the reference model is important. An objective function is built as follows:

$$J = \sqrt{\frac{1}{N} \left[\sum q \ddot{x}_s^2 + \sum qi (x_s - x_u)^2 + \sum (1-q) \ddot{x}_u^2 \right]} \quad (16)$$

where q is the weighting factor, i is the ratio factor, and N is the length of the sampling data.

According to the methods in document [20], by simulation and optimization, the damping coefficient of distribution β is chosen as 0.5, skyhook damping $C_{sh} = 3500\text{N}\cdot\text{s/m}$, groundhook damping $C_g = 3000\text{N}\cdot\text{s/m}$.

4.2. Joint Simulation

After the semi-active suspension multi-rigid-body model is output into Matlab through Adams/Controls, a simulation model for the semi-active suspension control system is built in combination with the Matlab/Simulink toolbox. Fig. (4) shows the simulation model of the model reference sliding mode control with fractional order reaching law. For comparison, the model reference sliding mode controller with an integer order reaching law (IOSMC) is designed. The general skyhook and groundhook hybrid controller (GHC) for the semi-active suspension is also designed. The suspension parameters are the same as those in the model reference fractional order sliding mode control, but a switch control is used. Moreover, a joint simulation model for passive suspension is designed. Passive damping

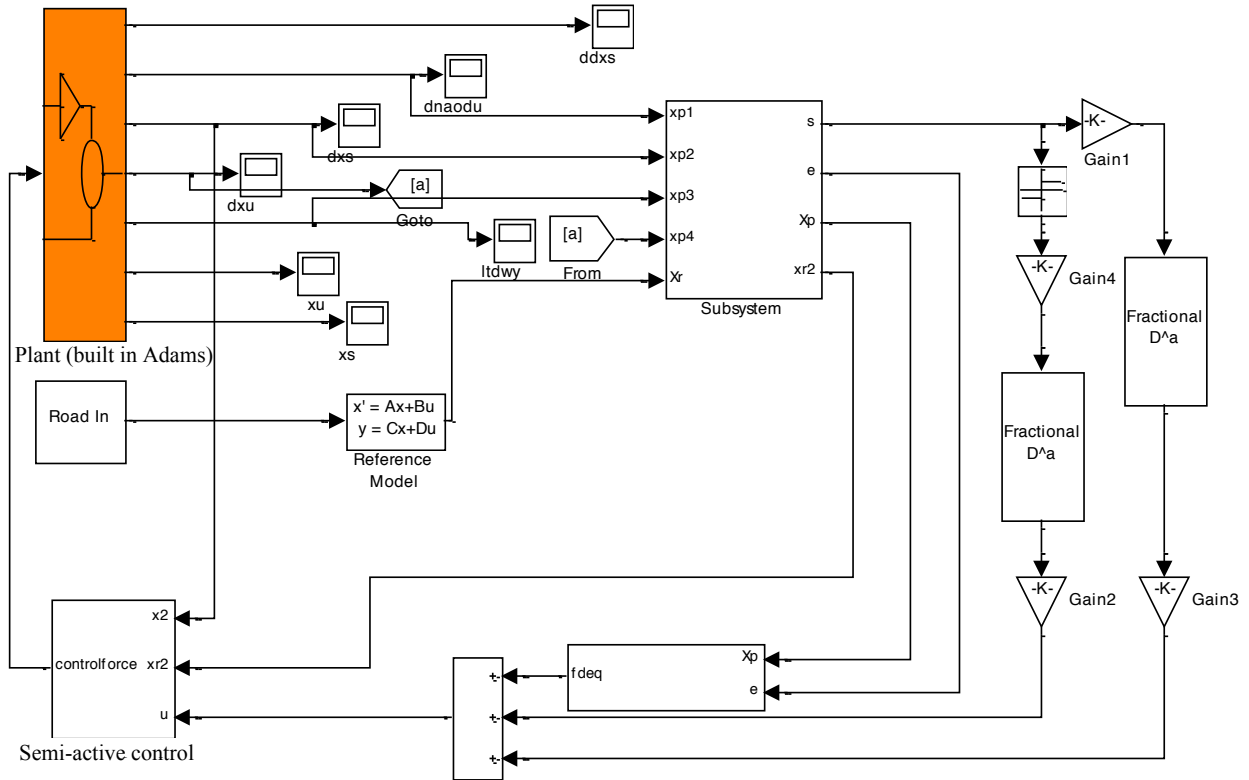


Fig. (4). Joint simulation model of fractional order model reference sliding mode control.

$c_p = 1800\text{N}\cdot\text{s}/\text{m}$. Figs. (5-7) show the power spectral density comparison charts of the sprung mass acceleration, suspension deflection, and tire deflection for four forms of suspension, respectively.

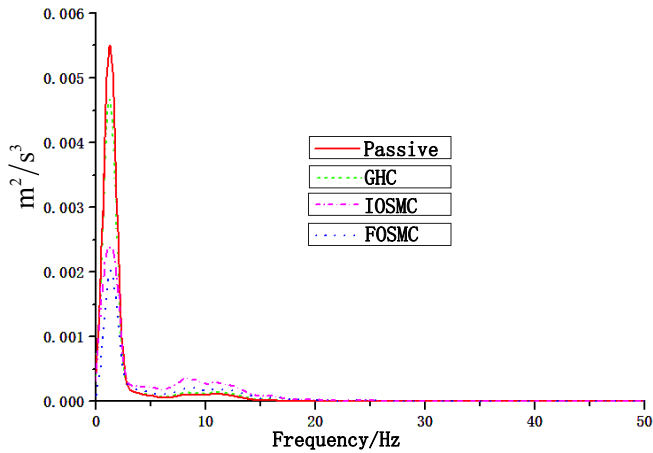


Fig. (5). Power spectral density of sprung mass acceleration.

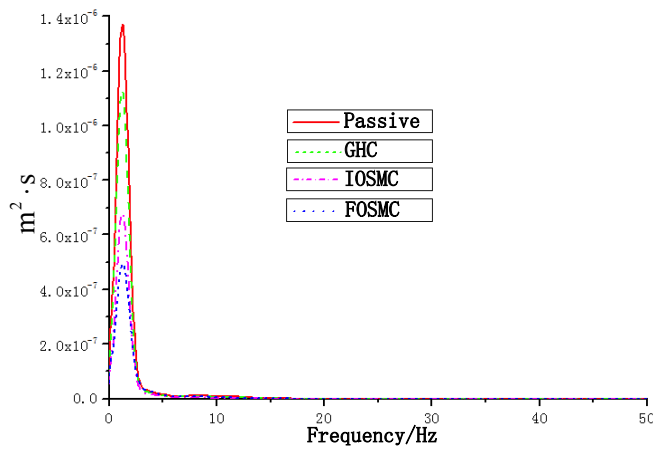


Fig. (6). Power spectral density of suspension deflection.

Fig. (5) shows the power spectral density comparison of the sprung mass acceleration. In the vicinity of the first natural frequency, the two controllers using the sliding mode control have a more substantial vibration reduction in amplitude than the general hybrid control and passive suspension. The sliding mode controller with fractional order exponential reaching law can suppress vibration better than the one with the integer order exponential reaching law. The passive suspension has the largest vibration. In the vicinity of the second-order natural frequency, three kinds of semi-active suspension have larger vibration peaks than passive

suspension. However, the sliding mode control with fractional order reaching law has smaller vibrations than the one with integer order reaching law and larger vibrations than the general hybrid control.

The power spectral density curves of suspension deflection, as shown in Fig. (6), indicates that it is similar to sprung mass acceleration in the vicinity of the first natural frequency. The two controllers using the sliding mode control have good control effects and a more substantial vibration reduction in amplitude than the general hybrid control and passive suspension. The vibration peak of the fractional order sliding mode control is minimal, and passive suspension has the largest vibration. In the vicinity of the second-order natural frequency, all vibration peaks are not obvious.

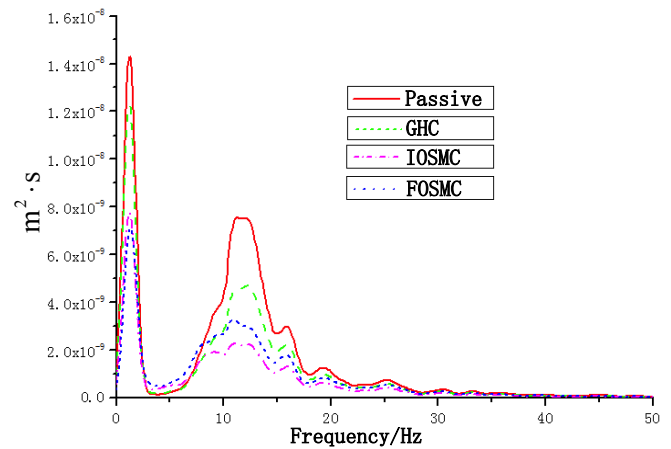


Fig. (7). Power spectral density of type deflection.

The power spectral density curves of the type deflection, as shown in Fig. (7), indicates that, in the vicinity of the first natural frequency, the semi-active suspension sliding mode control with the fractional order reaching law can greatly reduce the vibration peak and is better than the one with the integer order reaching law. The general hybrid controller has less effective control, and passive suspension has the largest vibration peak. In the vicinity of the second-order natural frequency, the sliding mode control with the fractional order reaching law and the control with the integer order reaching law both have better vibration inhibition effects. The amplitude of the former is larger than the one of the latter. Passive suspension has the largest peak.

To clearly show the simulation results of various forms of suspension, the list of the root mean square values is presented as follows:

Table 1. Comparison table of the root mean square values of each evaluation performance.

Susp. Type	Body Acc. (m/s ²)	Control Effect (%)	Susp. Def. (m)	Control Effect (%)	Type Def. (m)	Control Effect (%)
Passive	0.0955	-	0.0015	-	2.75E-4	-
GHC	0.0906	-5.13	0.0013	-13.33	2.38E-4	-13.45
IOSMC	0.0781	-18.25	0.0010	-33.33	2.20E-4	-20.18
FOSMC	0.0728	-23.77	9.45E-4	-37.0	2.13E-4	-22.55

CONCLUSION

Through the optimal design of the damping distribution ratio β in the optimally designed hybrid damping control strategy based on skyhook and groundhook, balance can be achieved between comfort and safety. A semi-active suspension model reference sliding mode controller with the fractional order exponential reaching law is designed according to this hybrid control as a reference model. The joint simulation of Adams and Matlab proves that the proposed controller has comprehensive control effectiveness that can reduce the tire dynamic load effectively and maintain better ride comfort. The exponent reaching law with fraction order calculus can improve the dynamic quality of the sliding mode motion. The proposed controller suppresses vibration better than the integer order exponential reaching law controller and has better performance than the general hybrid damping control strategy.

CONFLICT OF INTEREST

The author confirms that this article content has no conflict of interest.

ACKNOWLEDGEMENTS

This work is funded by The Overseas Training Program Foundation for University Excellent Young and Middle-aged Teachers and Presidents by Jiangsu Province, China Postdoctoral Science Foundation funded project (2011M500935), and the University Natural Science Foundation of Jiangsu Province (General Program) (grant number 11KJB580004).

REFERENCES

- [1] B Hredzak, S Gair, JF Eastham, Control of an EV drive with reduced unsprung mass, IEE Proceedings-Electric Power Applications, vol.145, no.6, pp.600-606, 1998.
- [2] D Hrovat, Influence of unsprung weight on vehicle ride quality, Journal of Sound and Vibration, vol.124, no.3, pp.497-516, 1988.
- [3] David J Purdy, Dave Simmer, Brief investigation into the effect on suspension motions of high unsprung mass, Journal of battlefield technology, vol.7, no.1, pp.15, 2004.
- [4] JF Eastham, MJ Balchin, T Betzer, HC Lai, S Gair, Disc motor with reduced unsprung mass for direct EV wheel drive, in: Industrial Electronics, 1995. ISIE'95., Proceedings of the IEEE International Symposium on, IEEE, 1995, pp. 569-573.
- [5] Go Nagaya, Yasumichi Wakao, Akihiko Abe, Development of an in-wheel drive with advanced dynamic-damper mechanism, JSAE review, vol.24, no.4, pp.477-481, 2003.
- [6] Andrés E Rojas Rojas, Haymo Niederkofler, Johann Willberger, Comfort and safety enhancement of passenger vehicles with in-wheel motors, in, SAE Technical paper, 2010.
- [7] Per Roger Johansen, Dean Patterson, Christopher O'Keefe, John Swenson, The use of an axial flux permanent magnet in-wheel direct drive in an electric bicycle, Renewable Energy, vol.22, no.1, pp.151-157, 2001.
- [8] Yee-Pien Yang, Yih-Ping Luh, Cheng-Huei Cheung, Design and control of axial-flux brushless DC wheel motors for electric vehicles-part I: Multiobjective optimal design and analysis, Magnetics, IEEE Transactions on, vol.40, no.4, pp.1873-1882, 2004.
- [9] Jianwen Guo, Surong Huang, Qi Zhang, Guodong Xie, Design of High Density AFIR Disc Wheel-motor, S&M Electric Machines, vol.31, no.6, pp.19-23, 2004.
- [10] Francesco Profumo, Zheng Zhang, Alberto Tenconi, Axial flux machines drives: a new viable solution for electric cars, Industrial Electronics, IEEE Transactions on, vol.44, no.1, pp.39-45, 1997.
- [11] PH Mellor, T Allen, D Howe, Hub-mounted electric drive-train for a high performance all-electric racing vehicle, 1996.
- [12] Guobao Ning, Research on Inhibition Method of Vertical Vibration Negative Influences Induced by In-wheel Motor Electric Vehicle, in, Tongji University, Shanghai, 2007.
- [13] Ying YANG, Gang LIU, Guang-yao ZHAO, Control Strategy Based on ADAMS Mechanical Model for Vehicle's Active Suspension and Simulation, Journal of Northeastern University (Natural Science), vol.27, no.1, pp.73-74, 2006.
- [14] Naizhou Wang, Research of sliding mode control based on fractional calculus, in, Nanjing Forestry University, Nanjing, 2010.
- [15] Weibing Gao, Theoretical Foundation for Variable Structure Control, China Science and Technology Press, 1990.
- [16] Igor Podlubny, Geometric and physical interpretation of fractional integration and fractional differentiation, arXiv preprint math/0110241, 2001.
- [17] S-B Choi, S-K Lee, Y-P Park, A hysteresis model for the field-dependent damping force of a magnetorheological damper, Journal of Sound and Vibration, vol.245, no.2, pp.375-383, 2001.
- [18] Dengzhu Fan, The Simulation and Test Research on the Control System of Semi-active Suspension equipped MR Damper, in, Nanjing Forestry University, Nanjing, 2007.
- [19] Makoto Yokoyama, J Karl Hedrick, Shigehiro Toyama, A model following sliding mode controller for semi-active suspension systems with MR dampers, in: American Control Conference, 2001. Proceedings of the 2001, IEEE, 2001, pp. 2652-2657.
- [20] Konghui Guo, Jinzhu Wang, Yaohua Guo, Bing Xue, Study on the Adjustability of Semi-active Suspension Based on Hybrid Damping Control, Automobile Technology, vol.2003, no.3, pp.1-5, 2013.

Received: May 26, 2015

Revised: July 14, 2015

Accepted: August 10, 2015

© Yao *et al.*; Licensee Bentham Open.

This is an open access article licensed under the terms of the (<https://creativecommons.org/licenses/by/4.0/legalcode>), which permits unrestricted, non-commercial use, distribution and reproduction in any medium, provided the work is properly cited.